

Electrical and dielectric behavior of MgO doped Ba_{0.7} Sr_{0.3} TiO₃ thin films on Al₂O₃ substrate

S. Y. Lee and T. Y. Tseng

Citation: *Applied Physics Letters* **80**, 1797 (2002); doi: 10.1063/1.1458067

View online: <http://dx.doi.org/10.1063/1.1458067>

View Table of Contents: <http://scitation.aip.org/content/aip/journal/apl/80/10?ver=pdfcov>

Published by the [AIP Publishing](#)

Articles you may be interested in

[Impact of Morphological Features on the Dielectric Breakdown at SiO₂/SiC Interfaces](#)

AIP Conf. Proc. **1292**, 47 (2010); 10.1063/1.3518308

[Optical and electrical properties of amorphous Gd_xGa_{0.4x}O_{0.6} films in Gd_xGa_{0.4x}O_{0.6}/Ga₂O₃ gate dielectric stacks on GaAs](#)

Appl. Phys. Lett. **84**, 2521 (2004); 10.1063/1.1695445

[Electrical properties of chemical-solution-derived Bi_{3.54}Nd_{0.46}Ti₃O₁₂ ferroelectric thin films](#)

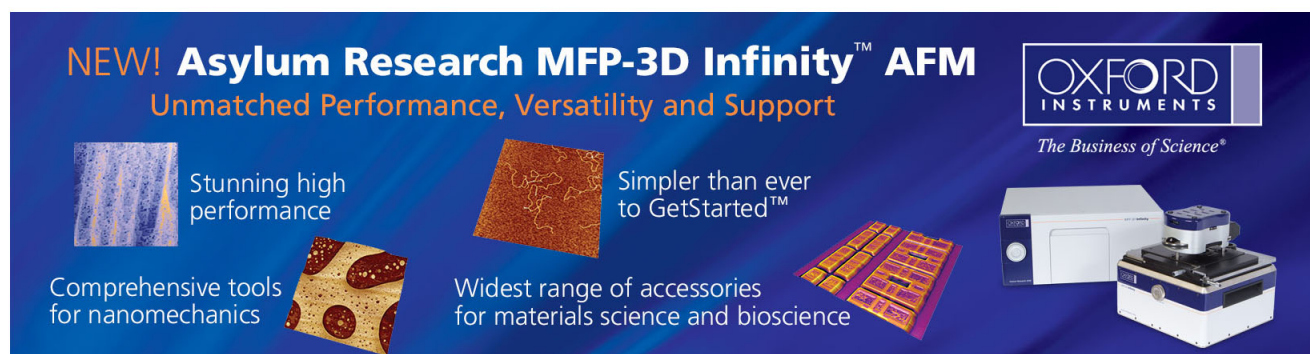
J. Appl. Phys. **94**, 7376 (2003); 10.1063/1.1622777

[Structural and electrical characteristics of the interfacial layer of ultrathin ZrO₂ films on partially strain compensated Si_{0.69}Ge_{0.3}C_{0.01} layers](#)

J. Vac. Sci. Technol. A **21**, 1758 (2003); 10.1116/1.1603279

[Nonlinear electrical behavior of the TiO₂/WO₃ varistor](#)

J. Appl. Phys. **92**, 4779 (2002); 10.1063/1.1503853



NEW! Asylum Research MFP-3D Infinity™ AFM
Unmatched Performance, Versatility and Support

OXFORD INSTRUMENTS
The Business of Science®

Stunning high performance

Simpler than ever to GetStarted™

Comprehensive tools for nanomechanics

Widest range of accessories for materials science and bioscience

Asylum Research

Electrical and dielectric behavior of MgO doped $\text{Ba}_{0.7}\text{Sr}_{0.3}\text{TiO}_3$ thin films on Al_2O_3 substrate

S. Y. Lee, and T. Y. Tseng^{a)}

Department of Electronics Engineering and Institute of Electronics, National Chiao-Tung University, Hsinchu 300, Taiwan, Republic of China

(Received 4 September 2001; accepted for publication 3 January 2002)

In this letter, we present the results of the fabrication and characterization of 5 mol % MgO doped $\text{Ba}_{0.7}\text{Sr}_{0.3}\text{TiO}_3$ (BST) films grown on Pt/TiN/ SiO_2 coated on Al_2O_3 substrates using the rf magnetron sputtering technique. The dielectric and electrical properties of $\text{Ba}_{0.7}\text{Sr}_{0.3}\text{TiO}_3$ thin film were found to improve obviously by means of MgO doping. The leakage current density of BST thin film decreased about 1 order of magnitude on MgO doping, while BST film with MgO doping had a higher dielectric constant than that without MgO doping. The dielectric constant of the films increased with increasing annealing temperature due to the consistent increase in grain size and crystallinity. The 750 °C annealed, 100 nm thick film indicated a high dielectric constant of 440 at 100 kHz and the lattice constant of 3.986 Å. The improvement of the electrical properties of BST films was associated with the reduced oxygen vacancies due to improved oxygenation of BST films in the presence of MgO. The MgO doped BST films exhibited a high tunability of 25% and dc resistivity of $6 \times 10^{10} \Omega \text{ cm}$ at an applied electric field of 200 kV/cm. The time-dependent dielectric breakdown studies indicated that the films had a longer lifetime of over 10 yrs on operation at the electric field of 0.4 MV/cm which is better than undoped BST film. © 2002 American Institute of Physics. [DOI: 10.1063/1.1458067]

The advancement of dynamic random access memories (DRAMs) has significantly decreased the available area per cell. Electroceramic thin films with high dielectric constant have attracted great attention for practical use in a capacitor of giga-bit DRAMs since the adoption of high dielectric constant materials can lower the height of the storage node and simplify the cell structure.^{1,2} One of the most promising materials for the capacitor dielectric film is $(\text{Ba}_{1-x}\text{Sr}_x)\text{TiO}_3$ (BST) because of its high dielectric constant, low leakage current density, high dielectric breakdown strength, relatively low dielectric relaxation time, low temperature coefficient of dielectric constant, the composition dependent Curie temperature, and paraelectric perovskite phase that does not exhibit fatigue, aging, and the ease of composition control due to the absence of volatile lead oxide.³

According to previous investigations, the electrical and dielectric properties and reliability of BST films heavily depend upon the thin film deposition method, composition, dopant, postannealed temperature, base electrode, microstructure, film thickness, surface roughness, oxygen content, and homogeneity of the film.⁴⁻⁶ Oxygen content in BST films has been identified to play an important role in determining the electrical and dielectric behavior of BST film. Inadequate oxygenation of BST films during growth in low oxygen partial pressure at elevated temperature may lead to the formation of oxygen vacancies, which act as charged traps. These charged traps leading to increased electron concentration affect the properties of BST film detrimentally.⁷ A suitable dopant can be used to decrease the concentration of electrons. In this letter, we report the improvement in elec-

trical properties of BST films by means of MgO doping. The dielectric constant, dielectric loss, and leakage current density of MgO doped BST films annealed at various temperatures were characterized with respect to measurement parameters such as applied electric field and measurement temperature. Experimental results indicate that the leakage current density of the BST film with 5 mol % MgO doping can be improved about 1 order of magnitude, while the dielectric constant of MgO doped film is 30% higher than that of undoped film.

In this letter, the undoped and 5 mol % MgO doped BST (Ba/Sr = 70/30) targets with a diameter of 2 in. and thickness of 1/4 in. were prepared using a standard solid-state powder-mixing reaction process. The sputtering chamber was evacuated to a base pressure of 2×10^{-6} Torr. All films were prepared at a fixed power of 100 W (the power density is 2.26 W/cm²) and constant pressure of 40 mTorr, which was maintained by a mixture of argon and oxygen at a mixing ratio of 1:1 with a total flow of 20 sccm. All BST films have the same thickness of around 100 nm. The substrate temperature was at 500 °C. The purpose of deposition of SiO_2 on the Al_2O_3 substrate was to improve surface roughness of the Al_2O_3 surface. The TiN layer was deposited between Pt and $\text{SiO}_2/\text{Al}_2\text{O}_3$ to enhance the interface adhesion and provide a diffusion barrier.

The grain size and film morphology analysis of the films were carried out by using atomic force microscopy (Digital Instruments Nano-Scope III) to reveal a simple dependence of grain growth on annealing temperature ranging from 550 to 750 °C in O_2 for 30 min in a rapid-thermal-annealing (RTA) furnace. The 50 nm thick Pt top electrode with a diameter of 250 μm was then formed by sputtering and patterned by the shadow mask process. The film thickness was

^{a)} Author to whom correspondence should be addressed; electronic mail: tseng@cc.nctu.edu.tw

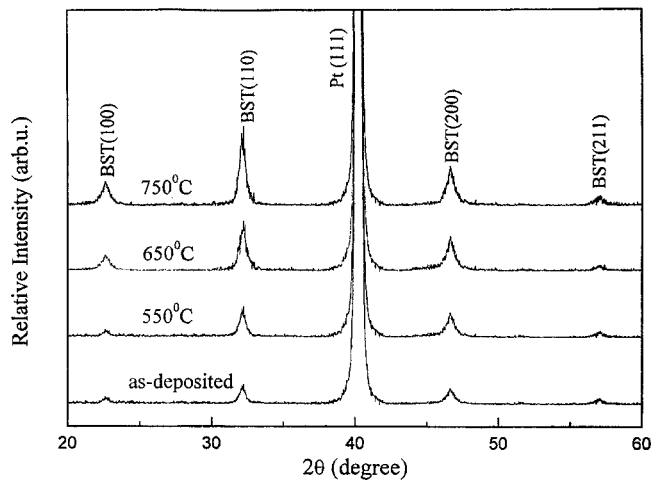


FIG. 1. XRD patterns of 5 mol % MgO doped BST films annealed in O_2 for 30 min at temperatures indicated.

determined from ellipsometry. The microstructural features of the films were examined by x-ray diffraction (XRD) (Siemens D5000). The dielectric and electrical measurements were conducted on the films in the metal–insulator–metal capacitor configuration. The leakage current of $Ba_{0.7}Sr_{0.3}TiO_3$ films was measured with a voltage step of 0.1 V and elapsed time of 30 s. The capacitance was measured at 100 kHz as a function of voltage from positive to negative bias. Dielectric constant of the films was calculated from the capacitance measured at 100 kHz without bias voltage. The dielectric properties were measured as a function of frequency with a HP 4194A impedance/gain phase analyzer. The insulating properties were evaluated from current–voltage and current–time measurements by measuring the current through the sample using HP 4156. The Pt top electrode of the BST capacitor was connected to the voltage source and the bottom electrode was ground.

Figure 1 shows the XRD patterns of the 50% OMR BST thin films doped with 5 mol % MgO deposited on Pt bottom electrodes at substrate temperature $500^\circ C$ and postannealed for 30 min at 550, 650, and $750^\circ C$ in O_2 ambient. The purpose of using 50% OMR is that the BST films with large grain size can exhibit large dielectric constants due to polarization of electric dipoles on the basis of a previous study.⁸ The oxygen stoichiometry also influences the dielectric constant of the films. The (110) peak intensity of the BST thin films becomes more intense in the XRD patterns with increasing temperature from 550 to $750^\circ C$ in O_2 ambient. It indicates from Fig. 1 that the crystallinity of those films is improved after the RTA process.

Figure 2 shows the variation of dielectric constant of both undoped and 5 mol % MgO doped BST thin films with RTA temperature. It depicts that the dielectric constant of MgO doped BST film is higher than that of undoped BST film at various RTA temperatures. The dielectric constant is related to oxygen stoichiometry, grain size, and crystallinity of the film. The average grain sizes of 5 mol % MgO doped as-deposited and $750^\circ C$ annealed BST films determined by Scherrer's formula are 417 and 493 Å, respectively, compared to undoped BST film, which are 378 and 436 Å under the same conditions. Therefore, the increase in dielectric constant may be attributed to the grain growth and improved

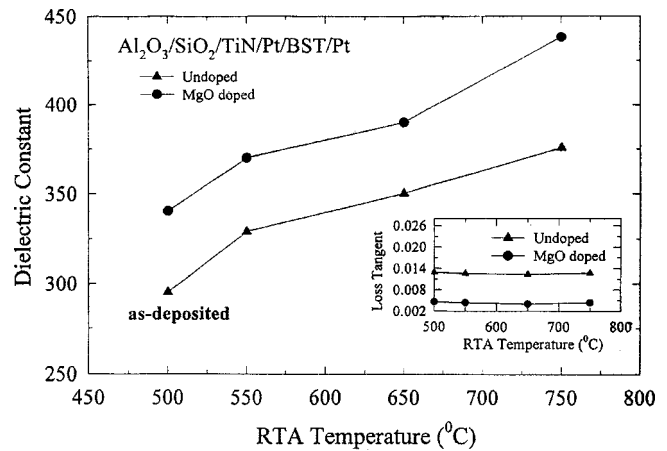


FIG. 2. Plots of dielectric constant vs annealing temperature for 5 mol % MgO doped and undoped BST film.

crystallinity of the films on the basis of the XRD result. From our experimental result, the dielectric constant and dissipation factor of the BST films are 390 and 0.004, respectively, while those of undoped BST films are 345 and 0.012, respectively, under being postannealed at $650^\circ C$ in an O_2 ambient. The better dielectric properties observed in MgO doped BST films are attributed to better crystallization, denser structure, and larger grain size compared to undoped BST film.

The root mean square surface roughnesses of MgO doped and undoped BST films increase with increasing annealing temperatures ranging from 550 to $750^\circ C$ (not shown here). The increasing surface roughness may be due to grain growth of annealed BST films. It can confirm this from the XRD data (Fig. 1) that the grain size increases with increasing annealing temperature. The MgO-doped films have higher surface roughnesses compared to undoped films, which is attributed to better crystallization and larger grain size of MgO doped films.

The difference in the leakage current characteristics of undoped and MgO-doped BST films is shown in Fig. 3. It is indicated that the leakage current density of MgO-doped BST film is about 1 order of magnitude lower than that of undoped BST films. Consider the addition of MgO into BST films. On the basis of the similarity in ionic radii between Mg^{2+} ($r_{eff}=0.72 \text{ \AA}$) and Ti^{4+} ($r_{eff}=0.61 \text{ \AA}$) in sixfold

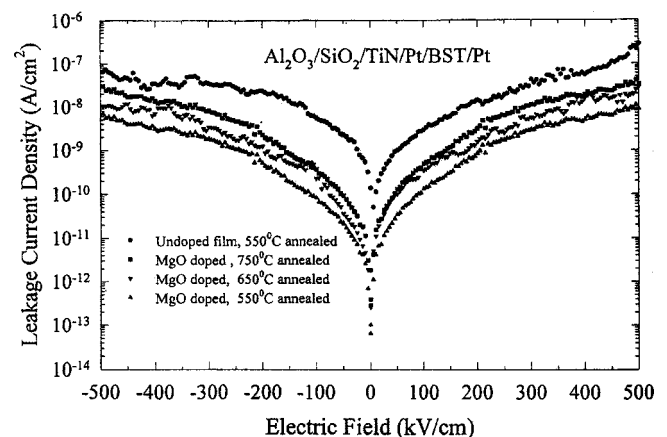
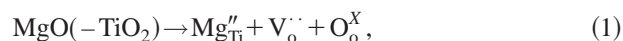


FIG. 3. Plots of leakage current density vs electric field for 5 mol % MgO doped and undoped BST film annealed at temperatures indicated.

coordination,⁹ it may be assumed that Mg replaces Ti in the BST lattice and a doubly ionized oxygen vacancy is simultaneously formed, i.e.,



where $\text{V}_{\text{O}}^{\cdot\cdot}$ is an extrinsic oxygen vacancy controlled by the Mg content. Mg behaves as an electron acceptor-type dopant, which can prevent reduction of Ti^{4+} to Ti^{3+} by neutralizing the donor action of the oxygen vacancies. In high temperature deposition of BST films under nonoxidizing atmosphere, such as Ar, generally produces oxygen vacancies in the film according to



where O_{O} , $\text{V}_{\text{O}}^{\cdot\cdot}$, and e' represent the oxygen ion on its normal site, oxygen vacancy, and electron, respectively. From Eqs. (1) and (2), it can be seen that both Mg_{Ti}'' and $\text{V}_{\text{O}}^{\cdot\cdot}$ are compensated for each other because they play the role of an acceptor and a donor in BST film, respectively. Oxygen vacancies created with MgO addition combined with the equilibrium reaction (2) requires that the concentration of electron be simultaneously decreased.

This decrease in electron concentration leads to lower leakage current of MgO doped BST film compared to undoped BST film. In Fig. 2, it is also indicated that 5 mol % MgO doped BST film has relatively low loss tangent compared to undoped BST film, which is consistent with the result of the lower leakage current of MgO-doped films shown in Fig. 3. The leakage current characteristics are distinctly similar in the positive and negative voltage region. The symmetry in positive and negative voltage parts of the J - E characteristic is due to the identical top and bottom electrode work functions in the two interfaces. It also implies that the leakage current is electrode limited.^{10,11} It is generally known that the leakage current of Pt/BST/Pt is controlled by Schottky barriers at the top BST/electrode and bottom BST/electrode interfaces. However, if these potential barriers are identical, then the J - E characteristics would be symmetric.

The leakage current density of the 550 °C annealed films is lower than those of 650 and 750 °C annealed films. The leakage current of BST film increases with increasing annealing temperature, which may be due to the enhanced ionic polarization and improved crystallinity with larger grain size. However, this enhanced ionic polarization would increase the energy dissipation during the relaxation,^{12,13} and films with large grain size also have short conduction paths along the highly resistive grain boundary, which cause an increase in the leakage current. This phenomenon implies that the higher dielectric constant and leakage current exhibited in the films annealed at temperatures above 550 °C may be attributed to their larger grain sizes. In our experiment, the leakage current density of MgO-doped BST film annealed at 650 °C for 30 min was 2×10^{-10} A/cm² at 100 kV/cm.

Figure 4 shows the lifetime extrapolation from dependence of cumulative failure on time-dependent dielectric breakdown (TDDB) stress time for the 100 nm thick films annealed at different temperatures. The TDDB studies indicate that all the films have a lifetime of over 10 yrs of op-

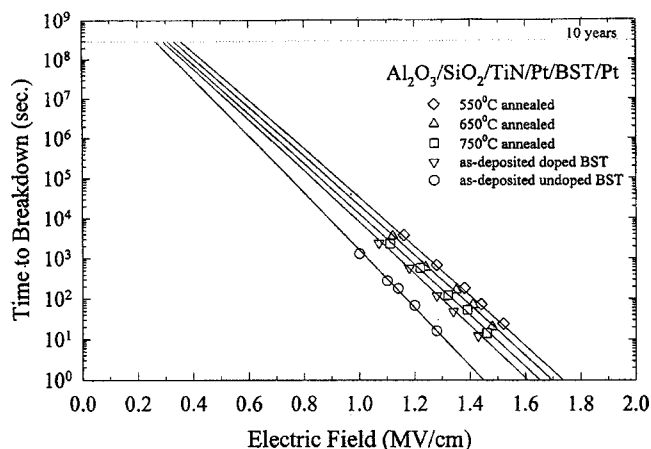


FIG. 4. TDDB lifetime as a function of electric field for 5 mol. % MgO doped films annealed at temperatures indicated and as-deposited undoped BST film.

eration at an electric field of 0.4 MV/cm. From Fig. 4, MgO doped BST films have a longer lifetime than undoped BST. The lifetime decreases with increasing annealing temperature.

In conclusion, our investigation demonstrated that MgO can be an effective dopant for increasing the dielectric constant, reducing the leakage current, and enhancing the reliability of $\text{Ba}_{0.7}\text{Sr}_{0.3}\text{TiO}_3$ thin films. We have shown that 550 °C annealed MgO doped BST film has a dielectric constant of 372, a loss tangent of 0.0037 at 100 kHz, a leakage current of 1×10^{-10} A/cm² at an electric field of 100 kV/cm, and a delay time 30 s, while 550 °C annealed undoped film has 329, 0.011, and 1×10^{-8} A/cm², respectively. Present studies suggest that the improved dielectric and insulating properties of MgO-doped BST films are suitable for tunable microwave and integrated capacitor applications.

The authors gratefully appreciate financial support from the National Science Council of the Republic of China under Project No. NSC 90-2212-E-009-029 and Cytect Co., Ltd, Hsinchu, Taiwan.

¹T. Horikawa, N. Mikami, T. Makita, J. Tanimura, M. Kataoka, K. Sato, and M. Nunoshita, *Jpn. J. Appl. Phys., Part 1* **32**, 4126 (1993).

²S. Ezhilvalavan and T. Y. Tseng, *Mater. Chem. Phys.* **65**, 227 (2000).

³M. Yamamuka, T. Kawahara, T. Makita, A. Yuuki, and K. Ono, *Jpn. J. Appl. Phys., Part 1* **35**, 729 (1996).

⁴C. S. Hwang, S. O. Park, H. J. Cho, C. S. Kang, H. K. Kang, S. I. Lee, and M. Y. Lee, *Appl. Phys. Lett.* **67**, 2819 (1995).

⁵M. S. Tsai and T. Y. Tseng, *IEEE Trans. CPMT* **23**, 128 (2000).

⁶Y. F. Kuo and T. Y. Tseng, *Electrochem. Solid-State Lett.* **2**, 236 (1996).

⁷T. S. Chen, V. Balu, B. Jiang, S. H. Kuah, J. C. Lee, P. Chu, R. E. Jones, P. Zurcher, D. J. Taylor, and S. Gillespie, *Integr. Ferroelectr.* **16**, 191 (1997).

⁸M. S. Tsai, S. C. Sun, and T. Y. Tseng, *J. Appl. Phys.* **82**, 3482 (1997).

⁹H. H. Wang, F. Chen, S. Y. Dai, T. Zhao, H. B. Lu, D. F. Cui, Y. L. Zhou, Z. H. Chen, and G. Z. Yang, *Appl. Phys. Lett.* **78**, 1676 (2001).

¹⁰S. Yamamichi, P. Y. Lesaicherre, H. Yamaguchi, K. Takemura, S. Sone, H. Yabuta, K. Sato, T. Tamura, K. Nakajima, S. Ohnishi, K. Tokashiki, Y. Hayashi, Y. Kato, Y. Miyasaka, M. Yoshida, and H. Ono, *IEEE Trans. Electron Devices* **44**, 1076 (1997).

¹¹K. Abe and S. Komatsu, *J. Appl. Phys.* **77**, 6461 (1995).

¹²J. Gerblinger and H. Meixner, *J. Appl. Phys.* **67**, 7453 (1990).

¹³M. Yoshida, H. Yamaguchi, T. Sakuma, and Y. Miyasaka, *J. Electrochem. Soc.* **142**, 244 (1995).